1   **The host factor ANP32A is required for influenza A virus vRNA and cRNA synthesis**

2

3   Benjamin E. Nilsson-Payant[1,#], Benjamin R. tenOever[1], Aartjan J.W. te Velthuis[2,3,#]

4

5   [1] Department of Microbiology, Icahn School of Medicine at Mount Sinai, New York, USA

6   [2] Division of Virology, Department of Pathology, University of Cambridge, Cambridge, UK

7   [3] Lewis Thomas Laboratory, Department of Molecular Biology, Princeton University, Princeton, USA

8

9   # Corresponding authors: benjamin.nilsson@mssm.edu; aj.te.velthuis@princeton.edu

10

11

12   Key words: RNA polymerase, influenza A virus, ANP32A, RNA replication,

13

14

ABSTRACT

Influenza A viruses are negative-sense RNA viruses that rely on their own viral replication machinery to replicate and transcribe their segmented single-stranded RNA genome. The viral ribonucleoprotein complexes in which viral RNA is replicated consist of a nucleoprotein scaffold around which the RNA genome is bound, and a heterotrimeric RNA-dependent RNA polymerase that catalyzes viral replication. The RNA polymerase copies the viral RNA (vRNA) via a replicative intermediate, called the complementary RNA (cRNA), and subsequently uses this cRNA to make more vRNA copies. To ensure that new cRNA and vRNA molecules are associated with ribonucleoproteins in which they can be amplified, the active RNA polymerase recruits a second polymerase to encapsidate the cRNA or vRNA. Host factor ANP32A has been shown to be essential for viral replication and to facilitate the formation of a dimer between viral RNA polymerases and differences between mammalian and avian ANP32A proteins are sufficient to restrict viral replication. It has been proposed that ANP32A is only required for the synthesis of vRNA molecules from a cRNA, but not vice versa. However, this view does not match recent molecular evidence. Here we use minigenome assays, virus infections, and viral promoter mutations to demonstrate that ANP32A is essential for both vRNA and cRNA synthesis. Moreover, we show that ANP32 is not only needed for the actively replicating polymerase, but also for the polymerase that is encapsidating nascent viral RNA products. Overall, these results provide new insights into influenza A virus replication and host adaptation.

IMPORTANCE

Zoonotic avian influenza A viruses pose a constant threat to global health and they have the potential to cause highly pathogenic pandemic outbreaks. Species variations in host factor ANP32A play a key role in supporting the activity of avian influenza A virus RNA polymerases in mammalian hosts. Here we show that ANP32A acts at two stages in the influenza A virus replication cycle, supporting recent structural experiments and in line with its essential role. Understanding how ANP32A supports viral RNA polymerase activity and how it supports avian polymerase function in mammalian hosts is important for understanding influenza A virus replication and the development of antiviral strategies against influenza A viruses.

INTRODUCTION

Influenza A viruses (IAV) are segmented negative-sense single-stranded RNA viruses that belong to the *Orthomyxoviridae*. IAV viruses infect a wide range of host species including humans, with wild aquatic birds being their natural reservoir (1). Humans are typically infected with seasonal, mammalian adapted IAV strains and only occasionally infected with avian adapted IAV strains. This is in part because zoonotic avian IAV strains are unable to efficiently transmit to and replicate in mammalian cells, unless multiple host species barriers are overcome (2). The two most important adaptations are i) a change in receptor binding specificity from α-2,3-linked sialic acids to α-2,6-linked sialic acids for effective viral entry into human cells (1), and ii) restored binding of the viral RNA-dependent RNA polymerase (RdRp) of avian IAV strains to host factor ANP32A for improved viral replication (3, 4).

The IAV RNA polymerase is composed of three subunits called polymerase basic 1 (PB1), PB2, and polymerase acidic (PA). The RNA polymerase replicates and transcribes the IAV genome segments in the context of viral ribonucleoprotein (vRNP) complexes (Fig 1A and 1B). In these vRNPs, the RNA polymerase binds to the ends of a single-stranded negative-sense viral RNA genome segment, while the viral nucleoprotein (NP) associates with the rest of the viral RNA (vRNA) segment in a double helical structure (5). During viral genome replication, vRNA segments are replicated by the viral RdRp through a complementary positive-sense RNA (cRNA) replicative intermediate, which requires at least one additional RNA polymerase to encapsidate the cRNA into a cRNP (5) (Fig 1A). The RNA polymerase in the cRNP next uses the cRNA as template to produce new vRNA genome segments, which is a process that requires at least one additional RdRp complex acting in a *trans*-activating capacity (5), and an RNA polymerase that encapsidates the vRNA into a new vRNP (6, 7) (Fig 1B).

One or more steps of avian-adapted IAV replication process are severely impaired in mammalian cells (2, 8), but a single glutamic acid-to-lysine mutation in the PB2 subunit (PB2-E627K) is sufficient to restore the activity of avian RNA polymerases in mammalian host cells (4). The molecular details underlying the impaired activity of avian RNA polymerases in mammalian cells are not fully understood, but several potential mechanisms have been proposed, including destabilized interactions of RNA polymerase and NP during vRNP assembly (9–12), reduced viral promoter RNA binding (13, 14), differential interactions with importin-α (15, 16), inhibitory or activating host factors (17, 18) and unstable cRNP structures of avian IAV in mammalian cells (19). However, expression of acidic (leucine-rich) nuclear phosphoprotein 32 family member A protein (ANP32A) from avian cells alone is sufficient to restore avian IAV RNA polymerase activity in mammalian cells (20), suggesting that the PB2-E627K mutation arises to compensate for an impaired interaction between mammalian ANP32A and the avian IAV RNA polymerase.

ANP32A consists of an N-terminal leucine-rich repeat (LRR) domain with four LRR motifs and a C-terminal low-complexity acidic region (LCAR) (21–23). Although the avian and mammalian ANP32A homologues have a high sequence identity, birds contain an additional exon duplication (24, 25). Alternative splicing of the avian ANP32A gene leads to three ANP32A proteins: one containing an additional SUMO

3

77 interaction motif (SIM)-like and LCAR sequence encoded by an additional exon; one containing an

78 additional LCAR sequencing through partial splicing of the additional exon; and one lacking the extra exon

79 and being similar to the mammalian ANP32A protein (25–27). Restoring avian IAV RdRp activity in

80 mammalian host cells by avian ANP32A overexpression was shown to be dependent on the presence of the

81 avian-specific exon duplication (20). ANP32A's closely related family member ANP32B, which is required for

82 mammalian cell-adapted RdRp function (28, 29), does not appear to play a role in restoring replication of

83 avian-adapted IAV (30).

84   Interaction studies of ANP32A and the viral RNA polymerase have suggested that ANP32A only

85 interacts with the complete heterotrimeric RNA polymerase (27, 28, 31, 32). ANP32A proteins containing

86 the avian signature exon duplication were also shown to have a much stronger affinity for the viral RNA

87 polymerase (26, 27, 33). Presence of the avian glutamic acid residue 627 (627E) on the PB2 subunit

88 significantly weakens the interaction with ANP32A, necessitating the additional ANP32A exon or PB2

89 mutation E627K to stabilize the interaction (34). The determinant of the differential interaction was mapped

90 to the C-terminal LCAR domain of ANP32A, which directly interacts with the flexible PB2 627-domain on

91 the viral RdRp (27, 33).

92   Interestingly, the interaction between ANP32A and the viral RNA polymerase is significantly

93 strengthened in the presence of viral RNA (26, 33), suggesting that ANP32A binds the RNA polymerase in

94 the context of an RNP. Recent cryo-electron microcopy structures of an influenza C virus RNA polymerase

95 dimer revealed that ANP32A formed a bridge between an RNA polymerase bound to RNA and an apo form

96 of the RNA polymerase (7), suggesting that ANP32A mediates the assembly of the viral replicase complex.

97 In line with this idea, ANP32A appears to be required for viral RNA genome replication, but not primary

98 transcription, in both avian and mammalian hosts (20, 28). Moreover, using recombinant purified protein,

99 human ANP32A has been shown to be an enhancer of vRNA synthesis by human-adapted IAV RNA

100 polymerases (28). Based on the latter observation, it has been proposed that ANP32A is only required for

101 the synthesis of vRNA molecules from a cRNA template, but not vice versa. However, both cRNA and vRNA

102 molecules are encapsidated and it is unlikely that IAV evolved separate encapsidation complexes for vRNA

103 and cRNA nascent strands.

104   To investigate at which stage in IAV replication ANP32A is critical, we used a combination of cell-

105 based minigenome assays, single-step promoter mutants, and recombinant IAV strains to systematically

106 characterize the role of ANP32A in IAV genome replication. We find that an IAV RNA polymerase with a

107 627E mutation is unable to efficiently synthesize both vRNA and cRNA, and that expression of avian ANP32A

108 is sufficient for the 627E RNA polymerase to restore both vRNA and cRNA synthesis. Overall, this study

109 provides new insights into the role of ANP32A in mediating IAV replicase function. Together these insights

110 lead to a better understanding of IAV genome replication and host adaptation.

111

112

4

RESULTS

Avian ANP32A stimulates infection and replication of IAV containing PB2 627E. Avian IAV RNA polymerase activity is significantly restricted in mammalian host cells (14, 17, 35) and it has been demonstrated that the expression of avian host protein ANP32A, but not ANP32B, is sufficient to restore avian IAV RNA polymerase activity in mammalian cells (20, 30). However, the exact step at which ANP32A is involved in RNA polymerase activity remains unclear. We set out to systematically analyze the role of ANP32A using PB2 627E as tool and exchanged the lysine of the mammalian-adapted influenza strain A/WSN/33 (H1N1) (abbreviated as WSN) with the avian-specific glutamic acid (WSN-K627E) using reverse genetics. As has been reported previously (17), the avian-like WSN-K627E virus was significantly restricted in both viral replication and transcription in human cells compared to WSN (Fig 2A). However, in avian cells, no significant difference in viral replication and transcription was observed between both viruses. To confirm that infection of human cells with the avian-like WSN-K627E virus would be restored by avian ANP32A, we transiently expressed chicken ANP32A (chANP32A) in HEK-293T cells and infected the cells with either wild-type WSN or avian-like WSN-K627E virus. While WSN-K627E was unable to grow in human cells in the absence of avian ANP32A, expression of chANP32A was sufficient to support WSN-K627E growth similar to the wild-type WSN virus (Fig 2B). Moreover, analysis of the accumulation of viral RNA in human cells showed that transient expression of chANP32A, but not human ANP32A (huANP32A), was able to fully restore restricted viral RNA synthesis by WSN-K627E, while exogenous expression of either chANP32A or huANP32A had no discernible effect on the replication of the wild-type WSN (Fig 2C).

Avian ANP32A stimulates replication, but not transcription by 627E-containing RNA polymerases. In order to confirm that the above observations are linked to the activity of the viral RNA polymerase and no other viral factors, we transiently reconstituted the minimal viral components necessary for genome transcription and replication in HEK-293T cells and analyzed the accumulation of the three viral RNA species cRNA, vRNA and mRNA. In agreement with the above findings, we found that vRNPs containing the PB2-627E subunit were significantly restricted in their activity, showing reduced production of all viral RNA species, and that viral RNA accumulation was restored in the presence of chANP32A (Fig 2D).

Accumulation of viral mRNA products is dependent on viral replication, which can confound analysis of the effect of ANP32A. As cellular protein translation is blocked by cycloheximide and protein translation is necessary for viral genome replication, but not transcription, cycloheximide can be used to obtain insight into primary transcription of incoming infecting vRNPs. To confirm that primary transcription by the 627E IAV vRNPs was independent of ANP32A in mammalian cells, we infected human HEK-293T cells at a high MOI with the WSN or WSN-K627E virus in the presence of cycloheximide. In agreement with previous reports, we found that there was no difference in mRNA synthesis, suggesting that the previously observed reduced mRNA levels were a consequence of impaired genome replication and consequently reduced vRNA template levels (Fig 2E).

5

149   The above result indicates that avian ANP32A is only required for the genome replication of avian-

150   like IAVs and not for their transcription. However, the findings do not prove that mammalian ANP32A plays

151   no role in the transcription of mammalian-adapted IAV RNA polymerases. Therefore, we knocked down

152   both human ANP32A and ANP32B, which have been shown to be redundant in mammalian cells (29), in

153   human alveolar epithelial A549 cells, and infected these cells with WSN at a high MOI. We found that early

154   in the infection cycle, no difference in primary transcription was observed in control and knockdown cells,

155   while a strong reduction in viral genome replication could be seen (Fig 2F and 2G). Overall, our findings

156   suggest that ANP32A is only involved in IAV replication and they confirm previous reports that an IAV RNA

157   polymerase with a 627E residue requires the presence of the avian ANP32A host factor to perform efficient

158   genome replication, but not transcription.

159

160   **The N-terminal third of ANP32A LCAR domain is required for efficient IAV replication.** An exon

161   duplication in the avian ANP32A gene was linked to the stimulation of avian IAV RNA polymerase (20, 24,

162   25). More recently, the central domain of ANP32A immediately upstream of the avian exon duplication was

163   linked to avian IAV RNA polymerase stimulation as well (30). In order to gain a better understanding of the

164   role of the ANP32A domains in IAV replication, internal and C-terminal deletions were introduced into a

165   chANP32A expression construct (Fig 3A and 3B). The ability of these truncated chANP32A proteins to

166   enhance viral replication by an avian-like RNA polymerase was determined using minigenome assays (Fig

167   3C). Deletion of the exon duplication in the chANP32A protein led to a loss in 627E RNA polymerase activity

168   relative to transient expression of the full-length chANP32A. However, in the presence of the exon

169   duplication a C-terminal or an internal truncation of 31 amino acids in the LCAR domain was compatible

170   with 627E RNA polymerase activity, while longer deletions of the LCAR domain led to a loss in 627E RNA

171   polymerase activity. Together, these results suggest that the LCAR domain of ANP32A plays a pivotal role

172   in supporting IAV RNA polymerase activity.

173

174   **Promoter binding is not restricted in avian RNPs.** Some reports have suggested that an avian RdRp

175   forms inherently weaker interactions with the vRNA template than a mammalian adapted IAV RdRp (13, 14).

176   The 627E residue is located far away from the promoter binding site and our previous work has shown that

177   the 627-domain does not affect the basic functions of the RNA polymerase (36). In an effort to exclude that

178   a single point mutation in PB2-627 leads to a significant difference in vRNA promoter binding and possible

179   vRNP assembly, the IAV RNA polymerase, either carrying a PB2-627K (K) or PB2-627E (E) subunit, a

180   catalytically inactive PB1 subunit (D445A/D446A) and a TAP-tagged PA subunit, was transiently expressed

181   in human HEK-293T cells together with a 76 nucleotide-long vRNA based on segment 5. Following

182   immunoprecipitation of the RNA polymerase, bound RNA was extracted and the amount of co-

183   immunoprecipitated vRNA was determined (Fig 4A). We observed that vRNA binding of a PB2-627E carrying

6

184   RNA polymerase was not impaired compared to a PB2-627K RNA polymerase. In addition, expression of
185   chANP32A did not have any impact on vRNA binding.

186   To get a more quantitative insight into vRNA and cRNA promoter binding activity of the mammalian
187   or avian-adapted IAV RNA polymerase, we performed single-molecule Förster resonance energy transfer
188   (sm-FRET) assays using recombinant catalytically inactive but RNA-binding competent RNA polymerases
189   and short fluorescently labelled viral RNA promoters. In an unbound state, both vRNA and cRNA promoters
190   form largely double-stranded RNA molecules (37) . However, if bound by the IAV RNA polymerase, the 5'
191   and 3' promoter ends are separated in space, which increases the distance between donor and acceptor
192   dyes (Fig 4B and 4C). We observed that the vRNA-bound FRET populations were similar, irrespective of
193   whether the RNA polymerase added to the vRNA carried a lysine or glutamic acid at position 627 or in fact
194   lacked the entire 627-domain (Fig 4D). Moreover, similar FRET populations, with a clear shift from the
195   unbound state, were observed for the cRNA promoter after addition of the different RNA polymerases (Fig
196   4E). Together, these data demonstrate that the 627-domain of the PB2 subunit does not play a role in vRNA
197   or cRNA promoter binding and that the nature of position PB2-627 has no impact on RNA polymerase-
198   RNA binding.

199

200   **ANP32A function in RNA polymerase activity is NP-independent.** The interaction between PB2 and NP
201   has been implicated several times as the cause for avian RNA polymerase restriction in mammalian cells (9–
202   12). Previously, it was reported that avian RNA polymerase activity was less diminished or even not
203   diminished on short viral RNA templates that do not require NP for viral replication (14). In order to
204   determine whether ANP32A's function is NP or vRNA template length dependent, we therefore transiently
205   expressed the IAV RNA polymerase in the presence or absence of NP and chANP32A together with a short
206   segment 5-based 76 nucleotide-long vRNA and analysed the accumulation of viral RNA in this NP-
207   independent minigenome assay (Fig 5A). We find that even in this NP-independent replication assay, the
208   PB2-K627E mutation led to a significant loss in RNA polymerase activity, which was restored in the presence
209   of chANP32A. The absence or presence of NP did not affect these results, suggesting that NP does not play
210   any major role in ANP32A function. Next, we tested whether using shorter vRNA templates affects ANP32A
211   function. Using both a 47 nucleotide-long (Fig 5B) and a 30 nucleotide-long (Fig 5C) segment 6-based vRNA
212   template we confirmed our observation that avian RNA polymerase restriction and the role of ANP32A in
213   IAV RNA replication is independent of both template length and NP.

214

215   **ANP32A is required for both cRNA and vRNA synthesis in mini genome assays.** Several studies have
216   suggested that a pair of mutations in the 3' vRNA promoter (G3A and C8U, Fig 6A) can improve avian RNA
217   polymerase activity in mammalian cells (13, 14). We wondered if we could use the RNA polymerase
218   promoter to uncouple vRNA synthesis and cRNA synthesis, and thus study at what step of viral replication
219   ANP32A is essential. This can only be addressed using minigenome assays, since both cRNA and vRNA

7

220   synthesis must occur during a viral infection. As a first step towards this aim, we performed minigenome

221   assays using either a construct expressing wild-type segment 6 vRNA or a segment 6 vRNA containing these

222   promoter mutations (3A8U), and found that viral replication was greatly enhanced by these promoter

223   mutations compared to the wild-type vRNA template (Fig 6B). However, even at elevated levels, replication

224   was still significantly, albeit less markedly, restricted by the 627E RNA polymerase. Additional expression of

225   chANP32A fully restored the activity of the 627E RNA polymerase, in line with our observations above.

226   Next, we introduced an additional mutation in the conserved 5′ vRNA stem-loop (G5U, Fig 6C) to

227   address whether the 3A8U mutation affects cRNA synthesis. The G5U mutation in the 5′ vRNA promoter

228   prevents internal initiation on the resulting cRNA product and therefore only allows primary mRNA as well

229   as primary cRNA synthesis but block subsequent vRNA synthesis and secondary transcription. This becomes

230   especially apparent when combining the G5U and 3A8U mutations (Fig 6D). Interestingly, minigenome

231   assays with vRNA templates carrying the G5U 5′ vRNA promoter mutation clearly demonstrated that the

232   627E RNA polymerase mutation prevented efficient primary cRNA synthesis. Activity of the 627E RNA

233   polymerase was restored by the additional expression of chANP32A (Fig 6E). These observations were

234   evident when using both the wild-type or the 3A8U 3′ vRNA promoter, lending further proof to our finding

235   that the 3A8U promoter mutation alone is not sufficient to overcome the restriction of the avian-like 627E

236   RNA polymerase.

237   In order to determine whether only cRNA synthesis or also vRNA synthesis is restricted in a 627E

238   RNA polymerase and whether ANP32A is required for efficient vRNA synthesis, we introduced a pair of

239   mutations (2C9G) in the 5′ cRNA promoter that would prevent 3′ terminal initiation on the resulting vRNA

240   product, thereby abolishing further cRNA synthesis, but not transcription (Fig 6F). Indeed, in a minigenome

241   assay no vRNA synthesis could be observed in the presence of the 2C9G cRNA template and the 627E RNA

242   polymerase (Fig 6G). Additional expression of chANP32A again was able to significantly increase RNA

243   polymerase activity.

244

245   **ANP32A is required for both cRNA and vRNA synthesis during infection.** In order to test whether these

246   results could be recapitulated in the context of an infection and whether avian RNA polymerase restriction

247   occurs at the level of the actively replicating RNA polymerase or at the level of a secondary RdRp necessary

248   to form nascent RNPs, we assessed the ability of an incoming vRNP to synthesize cRNA, and of the resulting

249   cRNP to perform further genome replication. Specifically, we pre-expressed either catalytically inactive

250   (PB1a) or active (wt) RNA polymerase, NP and chANP32A as indicated, before infecting cells with WSN in

251   the presence of the cellular transcription inhibitor Actinomycin D (Fig 6H). Therefore, viral replication is

252   entirely reliant on the presence of pre-expressed viral components. In the absence of IAV RNA polymerase,

253   no cRNA stabilization could be observed. Both PB2-627K or PB2-627E RNA polymerases were able to

254   stabilize nascent cRNA equally well when active replication by pre-expressed RNA polymerases was

255   prevented by the D445A/D446A mutation in the PB1 subunit. However, when further replication was

256 enabled by pre-expression of a catalytically active RNA polymerase, reduced levels of vRNA synthesis were
257 observed by the now actively replicating PB2-627E RNA polymerase, which was overcome by the addition
258 of chANP32A.

259 Overall, these results suggest that IAV RNA polymerases containing a PB2-K627E mutation are impaired at
260 the level of the actively replicating RNA polymerase and not the encapsidating RNA polymerase that is
261 required for nascent RNA binding. Furthermore, it also demonstrates that avian ANP32A is only required
262 for the actively replicating and not the encapsidating 627E RNA polymerase.

263
264

265 **DISCUSSION**

266 The RNA polymerase activity of avian IAV is significantly impaired in mammalian host cells and it has been
267 proposed that host factor ANP32A may restrict one step of the viral replication process. Here, we report
268 that ANP32A is required for both efficient vRNA as well as cRNA synthesis, but not viral transcription. This
269 is in agreement with previous studies (20, 28). In addition, we found that the N-terminal part of the LCAR
270 of ANP32A is critical for successful IAV RNA polymerase stimulation, in line with previous reports (27, 38).
271 Moreover, we show that the reduced activity of an IAV RNA polymerase containing PB2-627E in mammalian
272 cells is independent of vRNA or cRNA promoter binding, in contrast with previous reports that implicated
273 weaker promoter binding capabilities of avian-adapted RNA polymerases (13, 14). These findings clearly
274 confirm that ANP32A plays a more fundamental role in IAV genome. In addition, while a previous study
275 found that avian RdRp restriction was diminished or altogether abolished when using shorter vRNA
276 templates, we found that an inability to replicate vRNA templates remained, even when using templates of
277 30 nucleotides in length (14).

278 Our finding that avian-adapted RNA polymerases are able to stabilize nascent cRNA products
279 equally well in human host cells as mammalian-adapted RNA polymerases is in agreement with previous
280 studies (19, 36). However, here we additionally demonstrate that avian-adapted cRNPs are unable to
281 produce vRNA efficiently, suggesting that vRNA synthesis is impaired in the absence of the species-specific
282 ANP32A host protein. Furthermore, we also illustrate that not only vRNA synthesis is restricted, but that in
283 the context of minigenome assays, where only single-round replication cycles are permitted, both vRNA
284 and cRNA synthesis are inhibited by the PB2-K627E mutation and subsequently restored by the expression
285 of chANP32A. These data are consistent with recent structural findings where ANP32A is found to mediate
286 the assembly of the IAV replicase complex consisting of an actively replicating vRNP bound by ANP32A
287 which recruits an encapsidating RdRp (7).

288 In summary, these findings confirm that IAVs hijack ANP32A to facilitate viral genome replication
289 by mediating assembly of the replicase complex. It is tempting to speculate that IAVs evolved this
290 dependency in avian species. Because the mammalian ANP32A is shorter than its avian homologue, it
291 cannot efficiently support assembly of the IAV replicase complex at both stages of viral replication. Zoonotic

9

292   IAV strains must therefore acquire adaptive mutations to restore the ANP32A-RNA polymerase interaction.
293   These findings strengthen previous hypotheses about IAV host range restriction and shed further light on
294   the intricate details of IAV genome replication.

295

296

297   **MATERIALS AND METHODS**

298

299   **Cell Culture**.   Human alveolar basal epithelial carcinoma cells (A549, ATCC, CCL-185), human embryonic
300   kidney cells (HEK-293T, ATCC, CRL-3216), chicken embryonic fibroblasts (DF-1, ATCC, CRL-12203) and
301   Madin-Darby Canine kidney epithelial cells (MDCK, ATCC, CCL-34) were commercially obtained. All cells
302   were maintained at 37°C and 5% CO_2 in Dulbecco's Modified Eagle Medium (DMEM) supplemented with
303   10% Fetal Bovine Serum (FBS) and penicillin and streptomycin.

304

305   **Plasmids**.   Plasmids pcDNA-NP, pcDNA-PA, pcDNA-PB1, pcDNA-PB2, pcDNA-3a (45), pcDNA-PB1a (46),
306   pcDNA-PB2-K627E (10), pcDNA-PB2Δ535-667 (36), pcDNA-PA-TAP (47), pPOLI-NA (48), pPOLI-cNA (49),
307   pPOLI-NA47 (14), pPOLI-NP76 (50), as well as the pHW2000 constructs expressing the eight influenza
308   A/WSN/33 (H1N1) virus segments (51) have been described previously.
309   Plasmids pCMV-3xFLAG-GFP, pCMV-3xFLAG-huANP32A and pCMV-3xFLAG-chANP32A were generated by
310   InFusion cloning of coding sequences for GFP, huANP32A and chANP32A (synthesized by Integrated DNA
311   Technologies) into an empty pCMV-3Tag-1A vector (Agilent Technologies).
312   Plasmids pHW2000-PB2-K627E, pPOLI-NA-3A8U, pPOLI-NA-G5U, pPOLI-NA-3A8U/G5U and pPOLI-cNA-
313   2C9G were generated by site-directed PCR mutagenesis using the primers detailed in Table 1. Plasmids
314   pPOLI-NA30, pCMV-3xFLAG-chANP32AΔ180-208, pCMV-3xFLAG-chANP32AΔ209-281, pCMV-3xFLAG-
315   chANP32AΔ220-281, pCMV-3xFLAG-chANP32AΔ251-281 and pCMV-3xFLAG-chANP32AΔ220-250 were
316   generated by deletion PCR mutagenesis using primers detailed in Table 1.

317

318   **Virus infections**.   Recombinant influenza A/WSN/33 (H1N1) virus was generated using the pHW2000
319   eight-plasmid reverse genetics system as previously described (51). To generate a recombinant virus with
320   the avian signature lysine-to-glutamic acid point mutation at residue 627 of the PB2 segment, virus rescue
321   was performed with either the wild-type pHW2000-PB2 (WSN) or the mutated pHW2000-PB2-K627E (WSN-
322   K627E) segment.
323   For viral infections, approximately 1×10^6 human HEK-293T or chicken DF-1 cells were infected with WSN
324   or WSN-K627E at an MOI of 1 in DMEM supplemented with 0.5% FBS.
325   For analysis of primary viral transcription, infections were performed in the presence of 200 μg/ml
326   cycloheximide at an MOI of 10 in DMEM supplemented with 0.5% FBS.

327   For viral infections of transiently transfected cells, approximately 1×10^6 human HEK-293T cells were

328   transiently transfected with 1 μg of pCMV-3xFLAG-chANP32A, pCMV-3xFLAG-huANP32A or pCMV-

329   3xFLAG-GFP using Lipofectamine 2000 and Opti-MEM according to the manufacturer's instructions. 24 h

330   post-transfection, cells were infected at an MOI of 1 in DMEM supplemented with 0.5% FBS.

331   Total RNA was extracted from all infected samples at 6 h post-infection using TRIzol (Invitrogen) and

332   reconstituted in 20 μl nuclease-free water.

333

334   **Viral growth curves**.   Approximately 1×10^6 HEK-293T cells were transiently transfected with 1 μg of

335   pCMV-3xFLAG-chANP32A or pCMV-3xFLAG-GFP using Lipofectamine 2000 and Opti-MEM according to

336   the manufacturer's instructions. 24 h post-transfection, cells were infected with influenza A/WSN/33 (H1N1)

337   virus bearing either the wild-type PB2-627K or the avian signature PB2-627E amino acid residue at an MOI

338   of 0.001 in DMEM supplemented with 0.5% FBS. Cell culture media containing viral particles was collected

339   at 6, 24 and 48 h post-infection. The concentration of infectious viral particles (plaque-forming units/ml)

340   was determined by plaque assay on MDCK cells.

341

342   **RNP reconstitutions**.   In order to reconstitute vRNPs in a minigenome assay, approximately 1×10^6 HEK-

343   293T cells were transiently transfected with 1 μg of pcDNA-PA, pcDNA-PB1/pcDNA-PB1a, pcDNA-

344   PB2/pcDNA-PB2-K627E,   pcDNA-NP,   pCMV-3xFLAG-chANP32A/pCMV-3xFLAG-huANP32A/pCMV-

345   3xFLAG-GFP and a plasmid expressing a vRNA or cRNA segment (pPOLI-NA, pPOLI-cNA, pPOLI-NA-3A8U,

346   pPOLI-G5U, pPOLI-3A8U-G5U, pPOLI-cNA-2C9G) using Lipofectamine 2000 and Opti-MEM according to

347   the manufacturer's instructions. When using plasmids encoding short truncated vRNA templates (pPOLI-

348   NP76, pPOLI-NA47, pPOLI-NA30), transfections were performed in the absence of pcDNA-NP unless

349   otherwise stated. To ensure that equal amounts of DNA was transfected in all conditions, an empty pcDNA-

350   3a vector was used to balance the transfections. Total RNA was extracted 48 h post-transfection using TRIzol

351   (Invitrogen) and reconstituted in 20 μl of nuclease-free water.

352

353   **Primer extension analysis**.   The accumulation of viral mRNA, cRNA and vRNA was analyzed by primer

354   extension using ^{32}P-labelled primers specific for negative- or positive-sense segment 6 RNA as well as 5S

355   rRNA as an internal loading control as described previously (52). Primer sequences are detailed in Table 1.

356   Primer extension products were analyzed by 6% 7 M urea PAGE for full-length RNA templates or 12% 7 M

357   urea PAGE for truncated RNA templates and detected by autoradiography. ImageJ was used to analyze and

358   quantify ^{32}P-derived detected signal (53).

359

360   **siRNA-mediated knockdown of ANP32A/ANP32B**.   Approximately 1×10^6 A549 cells were transfected

361   with 20 nM ON-TARGETplus Non-Targeting Control Pool (Dharmacon, D-001810-10-20) or 20 nM

362   siGENOME Human ANP32A siRNA SMARTpool (Dharmacon, M-016060-00-0005) and siGENOME Human

11

363   ANP32B siRNA SMARTpool (Dharmacon, M-020148-01-0005) using Lipofectamine RNAiMax and Opti-

364   MEM according to the manufacturer's instructions. 48 h post-transfection, cells were either lysed for

365   Western blot analysis or infected with influenza A virus/WSN/33 (H1N1) virus.

366   For infections, cells were washed with PBS prior to infection, followed by infection with influenza A/WSN/33

367   (H1N1) virus at an MOI of 1 in DMEM supplemented with 0.3% BSA for 15 h. Total RNA was extracted using

368   TRIzol (Invitrogen) and reconstituted in 20 μl of nuclease-free water.

369

370   **Western blot analysis**.   For Western blot analysis, cells were lysed in NP-40 lysis buffer containing 1×

371   cOmplete Protease Inhibitor Cocktail (Roche) and 1× Phenylmethylsulfonyl fluoride (Sigma Aldrich) and

372   cleared from the insoluble fraction by centrifugation at 17,000 × g for 5 min at 4°C. Samples were analyzed

373   by SDS-PAGE and transferred onto nitrocellulose membranes. Membranes were probed with mouse

374   monoclonal anti-Actin (Thermo Scientific, MS-1295), mouse monoclonal anti-FLAG M2 (Sigma-Aldrich,

375   F1804), rabbit polyclonal anti-PHAP1 (Abcam, ab51013) and rabbit monoclonal anti-PHAPI2 (Abcam,

376   ab200836) antibodies. Primary antibodies were detected using HRP-conjugated secondary anti-mouse (GE

377   Healthcare, NA931V) and anti-rabbit (GE Healthcare, NA934V) antibodies and visualized using Immobilon

378   Western Chemiluminescent HRP substrate kit (Millipore) according to the manufacturer's instructions.

379

380

381   **RNA-binding assay**.   Approximately 1 × 10^6 HEK-293T cells were transiently transfected with 1 μg of

382   pcDNA-PA/pcDNA-PA-TAP, pcDNA-PB1a, pcDNA-PB2/pcDNA-PB2-K627E, pPOLI-NA47 and pCMV-

383   3xFLAG-chANP32A/pCMV-3xFLAG-GFP using Lipofectamine 2000 and Opti-MEM according to the

384   manufacturer's instructions. 48 h post-transfection, cells were lysed for 1 h at 4°C in 100 μl lysis buffer (50

385   mM Tris-HCl [pH=8.0], 150 mM NaCl, 0.5% NP-40, 1 mM DTT, 1 mM Phenylmethylsulfonyl fluoride, 1 mM

386   Na$_3$VO$_4$, 30 mM NaF, 10% glycerol, 1× cOmplete Protease Inhibitor Cocktail). After clarification of lysates

387   from cellular debris by centrifugation (17,000 x g, 5 min, 4°C), lysates were incubated for 24 h with

388   equilibrated IgG Sepharose 6 Fast Flow beads at 4°C. Beads were washed three times for 10 min at 4°C with

389   500 μl wash buffer (10 mM Tris-HCl [pH=8.0], 150 mM NaCl, 0.1% NP-40, 10% glycerol). Beads were

390   collected by centrifugation (17,000 x g, 5 min, 4°C) and supernatants were discarded. RNA was extracted

391   from whole cell lysates and IgG Sepharose beads using TRIzol and 20 μg GlycoBlue Coprecipitant

392   (Invitrogen) according to the manufacturer's instructions. RNA was analysed by primer extension and 12%

393   7M urea PAGE as described above.

394

395   **Recombinant RdRp purification and smFRET**.   Recombinant influenza A/WSN/33 (H1N1) polymerase

396   subunits containing a PB2 627K, 627E or delta 627 domain and a protein-A tag on the C-terminus of the PA

397   subunit were expressed in HEK-293T cells and purified using IgG-sepharose as described previously (54,

398   55). RNA and RNA polymerase were prepared and interactions between the molecules measured on a

399   custom-build confocal microscope as described previously. (54, 55)

400

401   **cRNA/vRNA stabilization assay**.   The ability of the viral RdRp to either stabilize nascent cRNA products

402   during primary viral replication or to facilitate replication of both vRNA and cRNA, was tested by transiently

403   transfecting approximately 1×10^6 HEK-293T cells with 1 μg of pcDNA-PA, pcDNA-PB1/pcDNA-PB1a,

404   pcDNA-PB2/pcDNA-PB2-K627E,   pcDNA-NP   and   pCMV-3xFLAG-chANP32A/pCMV-3xFLAG-GFP   as

405   indicated using Lipofectamine 2000 and Opti-MEM according to the manufacturer's instructions. 48 h post-

406   transfection, cells were infected with influenza A/WSN/33 (H1N1) virus in the presence of 5 μg/ml

407   Actinomycin D at an MOI of 5 in DMEM supplemented with 0.5% FBS. Total RNA was extracted 6 h post-

408   infection using TRIzol (Invitrogen) and reconstituted in 20 μl of nuclease-free water. The accumulation of

409   viral mRNA, cRNA and vRNA was analyzed by primer extension using ^{32}P-labelled primers specific for

410   negative- or positive-sense segment 6 RNA as well as 5S rRNA as an internal loading control as described

411   previously (52). Primer extension products were analyzed by 6% 7 M urea PAGE in TBE buffer and detected

412   by autoradiography. ImageJ was used to analyze and quantify ^{32}P-derived detected signal (53).

413

414

REFERENCES

1. Krammer F, Smith GJD, Fouchier RAM, Peiris M, Kedzierska K, Doherty PC, Palese P, Shaw ML, Treanor J, Webster RG, García-Sastre A. 2018. Influenza. Nat Rev Dis Prim 4:1–21.

2. Cauldwell A V., Long JS, Moncorgé O, Barclay WS. 2014. Viral determinants of influenza A virus host range. J Gen Virol 95:1193–1210.

3. Almond JW. 1977. A single gene determines the host range of influenza virus. Nature 270:617–618.

4. Kanta Subbarao E, London W, Murphy' BR. 1993. A Single Amino Acid in the PB2 Gene of Influenza A Virus Is a Determinant of Host Range. J Virol 67:1761–1764.

5. Fodor E, Velthuis AJWT. 2020. Structure and function of the influenza virus transcription and replication machinery. Cold Spring Harb Perspect Med 10:1–14.

6. te Velthuis AJW, Grimes JM, Fodor E. 2021. Structural insights into RNA polymerases of negative-sense RNA viruses. Nat Rev Microbiol. Nature Research.

7. Carrique L, Fan H, Walker AP, Keown JR, Sharps J, Staller E, Barclay WS, Fodor E, Grimes JM. 2020. Host ANP32A mediates the assembly of the influenza virus replicase. Nature 587:638–643.

8. Gabriel G, Fodor E. 2014. Molecular determinants of pathogenicity in the polymerase complex. Curr Top Microbiol Immunol 385:35–60.

9. Labadie K, Dos Santos Afonso E, Rameix-Welti MA, van der Werf S, Naffakh N. 2007. Host-range determinants on the PB2 protein of influenza A viruses control the interaction between the viral polymerase and nucleoprotein in human cells. Virology 362:271–282.

10. Ng AKL, Chan WH, Choi ST, Lam MKH, Lau KF, Chan PKS, Au SWN, Fodor E, Shaw PC. 2012. Influenza polymerase activity correlates with the strength of interaction between nucleoprotein and PB2 through the host-specific residue K/E627. PLoS One 7:e36415.

11. Rameix-Welti M-A, Tomoiu A, Dos Santos Afonso E, van der Werf S, Naffakh N. 2009. Avian Influenza A Virus Polymerase Association with Nucleoprotein, but Not Polymerase Assembly, Is Impaired in Human Cells during the Course of Infection. J Virol 83:1320–1331.

12. Hsia HP, Yang YH, Szeto WC, Nilsson BE, Lo CY, Ng AKL, Fodor E, Shaw PC. 2018. Amino acid substitutions affecting aspartic acid 605 and valine 606 decrease the interaction strength between the influenza virus RNA polymerase PB2'627' domain and the viral nucleoprotein. PLoS One 13.

13. Crescenzo-Chaigne B, Van der Werf S, Naffakh N. 2002. Differential effect of nucleotide substitutions in the 3' arm of the influenza A virus vRNA promoter on transcription/replication by avian and human polymerase complexes is related to the nature of PB2 amino acid 627. Virology 303:240–252.

14. Paterson D, te Velthuis AJW, Vreede FT, Fodor E. 2014. Host Restriction of Influenza Virus Polymerase Activity by PB2 627E Is Diminished on Short Viral Templates in a Nucleoprotein-Independent Manner. J Virol 88:339–344.

14

456   15.   Gabriel G, Klingel K, Otte A, Thiele S, Hudjetz B, Arman-Kalcek G, Sauter M, Shmidt T, Rother F,
457   Baumgarte S, Keiner B, Hartmann E, Bader M, Brownlee GG, Fodor E, Klenk HD. 2011. Differential
458   use of importin-α isoforms governs cell tropism and host adaptation of influenza virus. Nat
459   Commun 2.

460   16.   Hudjetz B, Gabriel G. 2012. Human-like PB2 627K influenza virus polymerase activity is regulated
461   by importin-α1 and -α7. PLoS Pathog 8.

462   17.   Mehle A, Doudna JA. 2008. An Inhibitory Activity in Human Cells Restricts the Function of an
463   Avian-like Influenza Virus Polymerase. Cell Host Microbe 4:111–122.

464   18.   Moncorgé O, Mura M, Barclay WS. 2010. Evidence for Avian and Human Host Cell Factors That
465   Affect the Activity of Influenza Virus Polymerase †. J Virol 84:9978–9986.

466   19.   Mänz B, Brunotte L, Reuther P, Schwemmle M. 2012. Adaptive mutations in NEP compensate for
467   defective H5N1 RNA replication in cultured human cells. Nat Commun 3:1–11.

468   20.   Long JS, Giotis ES, Moncorgé O, Frise R, Mistry B, James J, Morisson M, Iqbal M, Vignal A, Skinner
469   MA, Barclay WS. 2016. Species difference in ANP32A underlies influenza A virus polymerase host
470   restriction. Nature 529:101–104.

471   21.   Reilly PT, Yu Y, Hamiche A, Wang L. 2014. Cracking the ANP32 whips: Important functions, unequal
472   requirement, and hints at disease implications. BioEssays 36:1062–1071.

473   22.   Chen T-H, Brody JR, Romantsev FE, Yu J-G, Kayler AE, Voneiff E, Kuhajda FP, Pasternackt GR. 1996.
474   Structure of pp32, an Acidic Nuclear Protein Which Inhibits Oncogene-induced Formation of
475   Transformed Foci. Mol Biol Cell 7:2045–2056.

476   23.   Matilla A, Radrizzani M. 2005. The Anp32 family of proteins containing leucine-rich repeats.
477   Cerebellum 4:7–18.

478   24.   Baker SF, Ledwith MP, Mehle A. 2018. Differential Splicing of ANP32A in Birds Alters Its Ability to
479   Stimulate RNA Synthesis by Restricted Influenza Polymerase. Cell Rep 24:2581-2588.e4.

480   25.   Domingues P, Eletto D, Magnus C, Turkington HL, Schmutz S, Zagordi O, Lenk M, Beer M, Stertz S,
481   Hale BG. 2019. Profiling host ANP32A splicing landscapes to predict influenza A virus polymerase
482   adaptation. Nat Commun 10.

483   26.   Baker SF, Ledwith MP, Mehle A. 2018. Differential Splicing of ANP32A in Birds Alters Its Ability to
484   Stimulate RNA Synthesis by Restricted Influenza Polymerase. Cell Rep 24:2581-2588.e4.

485   27.   Domingues P, Hale BG. 2017. Functional Insights into ANP32A-Dependent Influenza A Virus
486   Polymerase Host Restriction. Cell Rep 20:2538–2546.

487   28.   Sugiyama K, Kawaguchi A, Okuwaki M, Nagata K. 2015. PP32 and APRIL are host cell-derived
488   regulators of influenza virus RNA synthesis from cRNA. Elife 4.

489   29.   Staller E, Sheppard CM, Neasham PJ, Mistry B, Peacock TP, Goldhill DH, Long JS, Barclay WS. 2019.
490   ANP32 Proteins Are Essential for Influenza Virus Replication in Human Cells. J Virol 93.

491   30.   Long JS, Idoko-Akoh A, Mistry B, Goldhill D, Staller E, Schreyer J, Ross C, Goodbourn S, Shelton H,

15

492   Skinner MA, Sang H, McGrew MJ, Barclay W. 2019. Species specific differences in use of ANP32
493   proteins by influenza A virus. Elife 8.

494 31. Bradel-Tretheway BG, Mattiacio JL, Krasnoselsky A, Stevenson C, Purdy D, Dewhurst S, Katze MG.
495   2011. Comprehensive Proteomic Analysis of Influenza Virus Polymerase Complex Reveals a Novel
496   Association with Mitochondrial Proteins and RNA Polymerase Accessory Factors. J Virol 85:8569–
497   8581.

498 32. York A, Hutchinson EC, Fodor E. 2014. Interactome Analysis of the Influenza A Virus
499   Transcription/Replication Machinery Identifies Protein Phosphatase 6 as a Cellular Factor Required
500   for Efficient Virus Replication. J Virol 88:13284–13299.

501 33. Mistry B, Long JS, Schreyer J, Staller E, Sanchez-David RY, Barclay WS. 2019. Elucidating the
502   Interactions between Influenza Virus Polymerase and Host Factor ANP32A. J Virol 94.

503 34. Camacho-Zarco AR, Kalayil S, Maurin D, Salvi N, Delaforge E, Milles S, Jensen MR, Hart DJ, Cusack
504   S, Blackledge M. 2020. Molecular basis of host-adaptation interactions between influenza virus
505   polymerase PB2 subunit and ANP32A. Nat Commun 11.

506 35. Massin P, van der Werf S, Naffakh N. 2001. Residue 627 of PB2 Is a Determinant of Cold Sensitivity
507   in RNA Replication of Avian Influenza Viruses. J Virol 75:5398–5404.

508 36. Nilsson BE, te Velthuis AJW, Fodor E. 2017. Role of the PB2 627 Domain in Influenza A Virus
509   Polymerase Function. J Virol 91.

510 37. Tomescu AI, Robb NC, Hengrung N, Fodor E, Kapanidis AN. 2014. Single-molecule FRET reveals a
511   corkscrew RNA structure for the polymerase-bound influenza virus promoter. Proc Natl Acad Sci U
512   S A 111:E3335–E3342.

513 38. Mistry B, Long JS, Schreyer J, Staller E, Sanchez-David RY, Barclay WS. 2019. Elucidating the
514   Interactions between Influenza Virus Polymerase and Host Factor ANP32A. J Virol 94.

515 39. Deng T, Vreede FT, Brownlee GG. 2006. Different De Novo Initiation Strategies Are Used by
516   Influenza Virus RNA Polymerase on Its cRNA and Viral RNA Promoters during Viral RNA
517   Replication. J Virol 80:2337–2348.

518 40. Jorba N, Area E, Ortín J. 2008. Oligomerization of the influenza virus polymerase complex in vivo. J
519   Gen Virol 89:520–524.

520 41. York A, Hengrung N, Vreede FT, Huiskonen JT, Fodor E. 2013. Isolation and characterization of the
521   positive-sense replicative intermediate of a negative-strand RNA virus. Proc Natl Acad Sci U S A
522   110.

523 42. Chang S, Sun D, Liang H, Wang J, Li J, Guo L, Wang X, Guan C, Boruah BM, Yuan L, Feng F, Yang M,
524   Wang L, Wang Y, Wojdyla J, Li L, Wang J, Wang M, Cheng G, Wang HW, Liu Y. 2015. Cryo-EM
525   Structure of Influenza Virus RNA Polymerase Complex at 4.3Å Resolution. Mol Cell 57:925–935.

526 43. Fan H, Walker AP, Carrique L, Keown JR, Serna Martin I, Karia D, Sharps J, Hengrung N, Pardon E,
527   Steyaert J, Grimes JM, Fodor E. 2019. Structures of influenza A virus RNA polymerase offer insight

16

528   into viral genome replication. Nature 573:287–290.

529   44.   Peng Q, Liu Y, Peng R, Wang M, Yang W, Song H, Chen Y, Liu S, Han M, Zhang X, Wang P, Yan J,

530   Zhang B, Qi J, Deng T, Gao GF, Shi Y. 2019. Structural insight into RNA synthesis by influenza D

531   polymerase. Nat Microbiol 4:1750–1759.

532   45.   Fodor E, Crow M, Mingay LJ, Deng T, Sharps J, Fechter P, Brownlee GG. 2002. A Single Amino Acid

533   Mutation in the PA Subunit of the Influenza Virus RNA Polymerase Inhibits Endonucleolytic

534   Cleavage of Capped RNAs. J Virol 76:8989–9001.

535   46.   Vreede FT, Jung TE, Brownlee GG. 2004. Model Suggesting that Replication of Influenza Virus Is

536   Regulated by Stabilization of Replicative Intermediates. J Virol 78:9568–9572.

537   47.   Deng T, Sharps J, Fodor E, Brownlee GG. 2005. In Vitro Assembly of PB2 with a PB1-PA Dimer

538   Supports a New Model of Assembly of Influenza A Virus Polymerase Subunits into a Functional

539   Trimeric Complex. J Virol 79:8669–8674.

540   48.   Fodor E, Devenish L, Engelhardt OG, Palese P, Brownlee GG, García-Sastre A. 1999. Rescue of

541   Influenza A Virus from Recombinant DNA. J Virol 73:9679–9682.

542   49.   Vreede FT, Gifford H, Brownlee GG. 2008. Role of Initiating Nucleoside Triphosphate

543   Concentrations in the Regulation of Influenza Virus Replication and Transcription. J Virol 82:6902–

544   6910.

545   50.   Turrell L, Lyall JW, Tiley LS, Fodor E, Vreede FT. 2013. The role and assembly mechanism of

546   nucleoprotein in influenza A virus ribonucleoprotein complexes. Nat Commun 4:1591.

547   51.   Hoffmann E, Neumann G, Kawaoka Y, Hobom G, Webster RG. 2000. A DNA transfection system for

548   generation of influenza A virus from eight plasmids. Proc Natl Acad Sci 97:6108–6113.

549   52.   Nilsson-Payant BE, Sharps J, Hengrung N, Fodor E. 2018. The Surface-Exposed PA 51-72 -Loop of

550   the Influenza A Virus Polymerase Is Required for Viral Genome Replication. J Virol 92.

551   53.   Schneider CA, Rasband WS, Eliceiri KW. 2012. NIH Image to ImageJ: 25 years of image analysis. Nat

552   Methods 9:671–675.

553   54.   Te Velthuis AJW, Robb NC, Kapanidis AN, Fodor E. 2016. The role of the priming loop in influenza

554   A virus RNA synthesis. Nat Microbiol 1:1–7.

555   55.   Robb NC, Te Velthuis AJW, Wieneke R, Tampe R, Cordes T, Fodor E, Kapanidis AN. 2016. Single-

556   molecule FRET reveals the pre-initiation and initiation conformations of influenza virus promoter

557   RNA. Nucleic Acids Res 44:10304–10315.

558

559

FIGURE LEGENDS

FIG 1   Influenza A virus genome replication. **(A)** Schematic of vRNA-to-cRNA replication by the resident RNA polymerase in vRNPs. Nascent cRNA is encapsidated by a newly synthesized RNA-free polymerase. **(B)** Schematic of cRNA-to-vRNA replication by the resident RNA polymerase aided by a second regulatory polymerase. Nascent vRNA is being encapsidated by a newly synthesized RNA-free polymerase.

FIG 2   ANP32A is required for IAV genome replication. **(A)** Human HEK-293T cells or chicken DF-1 cells were infected with influenza A/WSN/33 (H1N1) virus carrying either a lysine (K) or glutamic acid (E) on residue 627 of the PB2 subunit for 6 h at an MOI of 1. The accumulation of viral RNA was analyzed by primer extension and 6% PAGE. The graph shows the relative mean intensity of viral RNA normalized to 5S rRNA from three independent biological replicates. **(B)** HEK-293T cells were transiently transfected with plasmids expressing GFP or chANP32A. 24 h post-transfection, cells were infected with mammalian- (K) or avian- (E) adapted influenza A/WSN/33 (H1N) at an MOI of 0.01. Infectious viral titers were determined by plaque assay at the indicated timepoints post-infection from three independent biological replicates. **(C)** HEK-293T cells were transfected with plasmids expressing huANP32A or chANP32A or GFP as a negative control. 24h post-transfection, cells were infected with wild-type influenza A/WSN/33 (H1N1) virus (WSN) or virus with a PB2-K627E mutation (WSN-K627E) at an MOI of 1 for 6 h. The accumulation of viral RNA was analyzed by primer extension and 6% PAGE. The graph shows the relative mean intensity of viral RNA normalized to 5S rRNA from three independent biological replicates. **(D)** HEK-293T cells were transfected with plasmids expressing NP, PA, PB1, PB2 (627K or 627E), segment 6 vRNA and huANP32A, chANP32A or GFP. 48h post-transfection, the accumulation of viral RNA was analyzed by primer extension and 6% PAGE. The graph shows the relative mean intensity of viral RNA normalized to 5S rRNA from three independent biological replicates. **(E)** HEK-293T cells were infected with wild-type influenza A/WSN/33 (H1N1) virus (WSN) or virus with a PB2-K627E mutation (WSN-K627E) at an MOI of 10 for 6 h in the presence of cycloheximide. The accumulation of viral RNA was analyzed by primer extension and 6% PAGE. The graph shows the relative mean intensity of viral RNA normalized to 5S rRNA from three independent biological replicates. **(F-G)** A549 cells were transfected with siRNA targeting human ANP32A and ANP32B. 48 h post-transfection cells were either (**F**) lysed for Western blot analysis for ANP32A and ANP32B expression or (**G**) infected with influenza A/WSN/33 (H1N1) virus (WSN) at an MOI of 1 for 12 h. The accumulation of viral RNA was analyzed by primer extension and 6% PAGE. Error bars represent the standard deviation of the means and asterisks represent a significant difference from the control group (two-tailed one-sample t test) as follows: ns, $P >$ 0.05; *, $P < 0.05$; **, $P < 0.01$; ***, $P < 0.001$; ****, $P < 0.0001$.

FIG 3   The chANP32A LCAR domain is essential for avian RdRp stimulation. **(A)** Schematic of the wild-type chANP32A protein and the internal and terminal truncations introduced in this study. **(B)** HEK-293T

18

596   cells were transfected with plasmids expressing NP, PA, PB1, PB2 or PB2-K627E, segment 6 vRNA and either

597   wild-type or truncated chANP32A. 48h post-transfection, the accumulation of viral RNA was analyzed by

598   primer extension and 6% PAGE. The graph shows the relative mean intensity of viral RNA normalized to 5S

599   rRNA from three independent biological replicates. Error bars represent the standard deviation of the means

600   and asterisks represent a significant difference from the control group (two-tailed one-sample t test) as

601   follows: ns, $P > 0.05$; *, $P < 0.05$; **, $P < 0.01$; ***, $P < 0.001$; ****, $P < 0.0001$.

602

603   **FIG 4**   The PB2 627-domain does not affect viral RNA binding. **(A)** HEK-293T cells were transfected with

604   plasmids expressing PA, PB2 (627K or 627E), catalytically inactive PB1, a 47 nucleotide-long internally

605   truncated segment 6 and where indicated chANP32A. 48 h post-transfection, cells were lysed and the viral

606   RdRp was immunoprecipitated via a TAP-tag on PA. Co-precipitated vRNA was analyzed by primer

607   extension and 12% PAGE. **(B)** Schematic of the influenza A virus vRNA promoter before and after binding

608   with the viral RdRp. The distance between the Atto647N dye (red) and the Cy3 dye (orange) is indicated.

609   **(C)** Schematic of the influenza A virus cRNA promoter before and after binding with the viral RdRp. The

610   distance between the Atto647N dye (red) and the Cy3 dye (orange) is indicated. **(D)** vRNA promoter

611   binding by the influenza A virus RdRp as analyzed by smFRET. Recombinant viral RdRp, either with a PB2

612   subunit with a lysing (627K) or glutamic acid (627E) at position 627 or with a subunit lacking the entire 627-

613   domain (Δ535-667) was used. The FRET populations were fit with a single Gaussian curve. The RNA only

614   (red) is shown as comparison. The means of the bound (black dotted line) and unbound (red dotted line)

615   signal is indicated in each graph. **(E)** cRNA promoter binding by the influenza A virus RdRp as analyzed by

616   smFRET. Recombinant viral RdRp, either with a PB2 subunit with a lysing (627K) or glutamic acid (627E) at

617   position 627 or with a subunit lacking the entire 627-domain (Δ535-667) was used. The FRET populations

618   were fit with a double Gaussian curve representing the two conformations that the cRNA promoter adopts

619   in a pre-initiation state. The unbound RNA only (red line) is shown as comparison.

620

621   **FIG 5**   Avian RdRp restriction in mammalian cells is independent of NP. **(A)** HEK-293T cells were

622   transfected with plasmids expressing a 76 nucleotide-long internally truncated segment 5 vRNA, PA, PB1,

623   PB2 and where indicated NP and chANP32A. 48 h post-transfection, the accumulation of viral RNA was

624   analyzed by primer extension and 12% PAGE. **(B)** HEK-293T cells were transfected with plasmids expressing

625   a 47 nucleotide-long internally truncated segment 6 vRNA, PA, PB1, PB2 and where indicated chANP32A.

626   48 h post-transfection, the accumulation of viral RNA was analyzed by primer extension and 12% PAGE.

627   The graph shows the relative mean intensity of viral RNA normalized to 5S rRNA from three independent

628   biological replicates. **(C)** HEK-293T cells were transfected with plasmids expressing a 30 nucleotide-long

629   internally truncated segment 6 vRNA, PA, PB1, PB2 and where indicated chANP32A. 48 h post-transfection,

630   the accumulation of viral RNA was analyzed by primer extension and 12% PAGE. The graph shows the

631   relative mean intensity of viral RNA normalized to 5S rRNA from three independent biological replicates.

19

632 Error bars represent the standard deviation of the means and asterisks represent a significant difference

633 from the control group (two-tailed one-sample t test) as follows: ns, $P > 0.05$; *, $P < 0.05$; **, $P < 0.01$; ***, P

634 < 0.001; ****, $P < 0.0001$.

635

636 **FIG 6** ANP32A is required for both vRNA and cRNA synthesis. **(A)** Schematic of the wild-type vRNA

637 promoter or a vRNA promoter carrying a G3A and C8U mutation in the 3′ vRNA promoter (red). **(B)** HEK-

638 293T cells were transfected with plasmids expressing NP, PA, PB1, PB2 (627K or 627E), segment 6 vRNA and

639 chANP32A where indicated. 48h post-transfection, the accumulation of viral RNA was analyzed by primer

640 extension and 6% PAGE. The graph shows the relative mean intensity of viral RNA produced from the

641 mutant 3A8U vRNA template normalized to 5S rRNA from three independent biological replicates. **(C)**

642 Schematic of the vRNA promoter carrying a G5U mutation in the 5′ vRNA promoter with and without the

643 3A8U 3′ vRNA promoter mutation. **(D)** HEK-293T cells were transfected with plasmids expressing NP, PA,

644 PB1, PB2 (627K or 627E), segment 6 vRNA and chANP32A where indicated. 48h post-transfection, the

645 accumulation of viral RNA was analyzed by primer extension and 6% PAGE. The graph shows the relative

646 mean intensity of cRNA normalized to 5S rRNA from three independent biological replicates. **(E)** Schematic

647 of the wild-type cRNA promoter or a cRNA promoter carrying a G2C and C9G mutation in the 5′ cRNA

648 promoter. **(F)** HEK-293T cells were transfected with plasmids expressing NP, PA, PB1, PB2 (627K or 627E),

649 segment 6 cRNA and chANP32A where indicated. 48h post-transfection, the accumulation of viral RNA was

650 analyzed by primer extension and 6% PAGE. The graph shows the relative mean intensity of vRNA produced

651 from the mutant 2C9G cRNA template normalized to 5S rRNA from three independent biological replicates.

652 **(G)** HEK-293T cells were transfected with NP, PA, PB1 or catalytically inactive PB1a, PB2 (627K or 627E) and

653 chANP32A where indicated. 24 h post-transfection, cells were infected with influenza A/WSN/33 (H1N1)

654 virus at an MOI of 5 for 6 h in the presence of Actinomycin D. The accumulation of viral RNA was analyzed

655 by primer extension and 6% PAGE. The graph shows the relative mean intensity of viral RNA normalized to

656 5S rRNA from four independent biological replicates. Error bars represent the standard deviation of the

657 means and asterisks represent a significant difference from the control group (two-tailed one-sample t test)

658 or between two non-control groups (two-tailed two-sample t test) as follows: ns, $P > 0.05$; *, $P < 0.05$; **, P

659 < 0.01; ***, $P < 0.001$; ****, $P < 0.0001$.
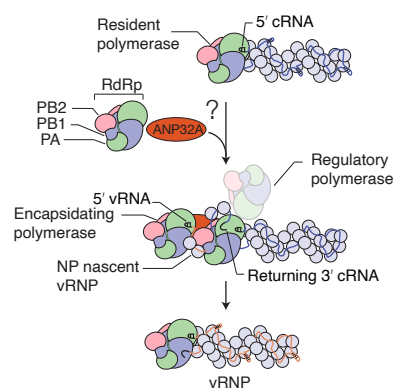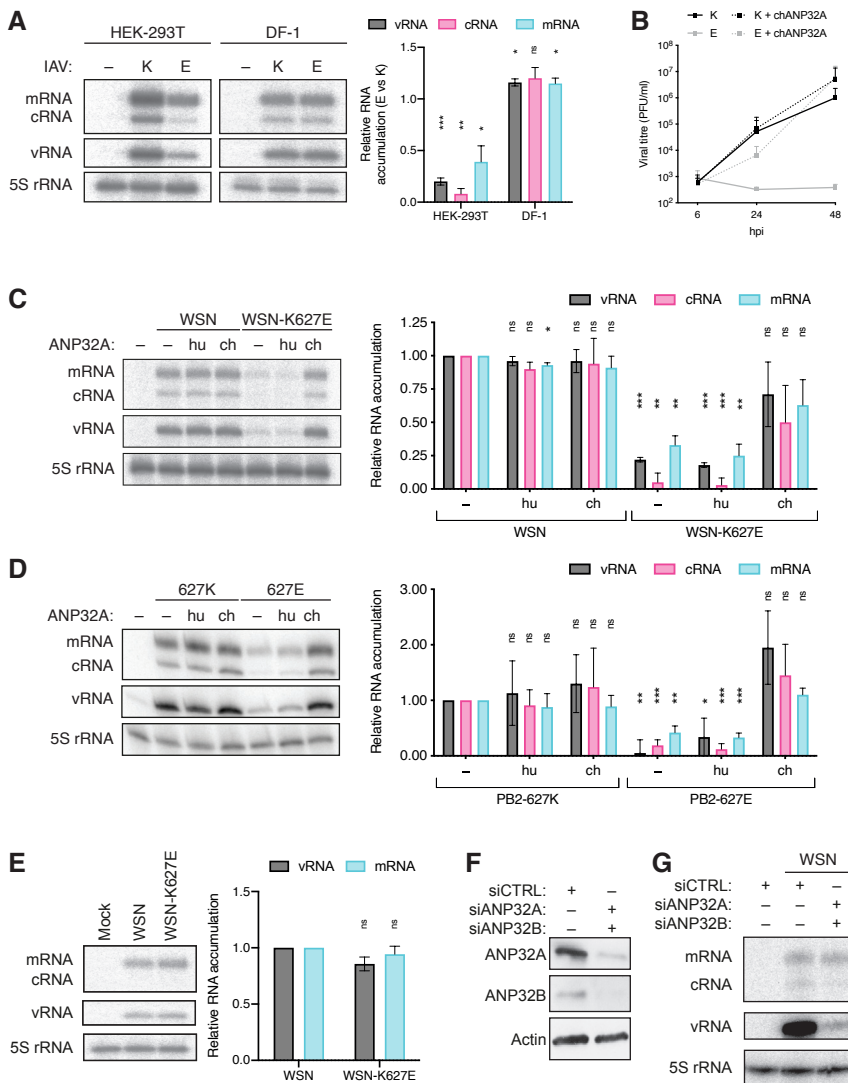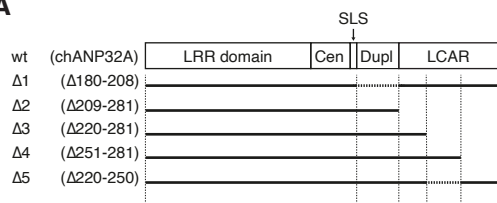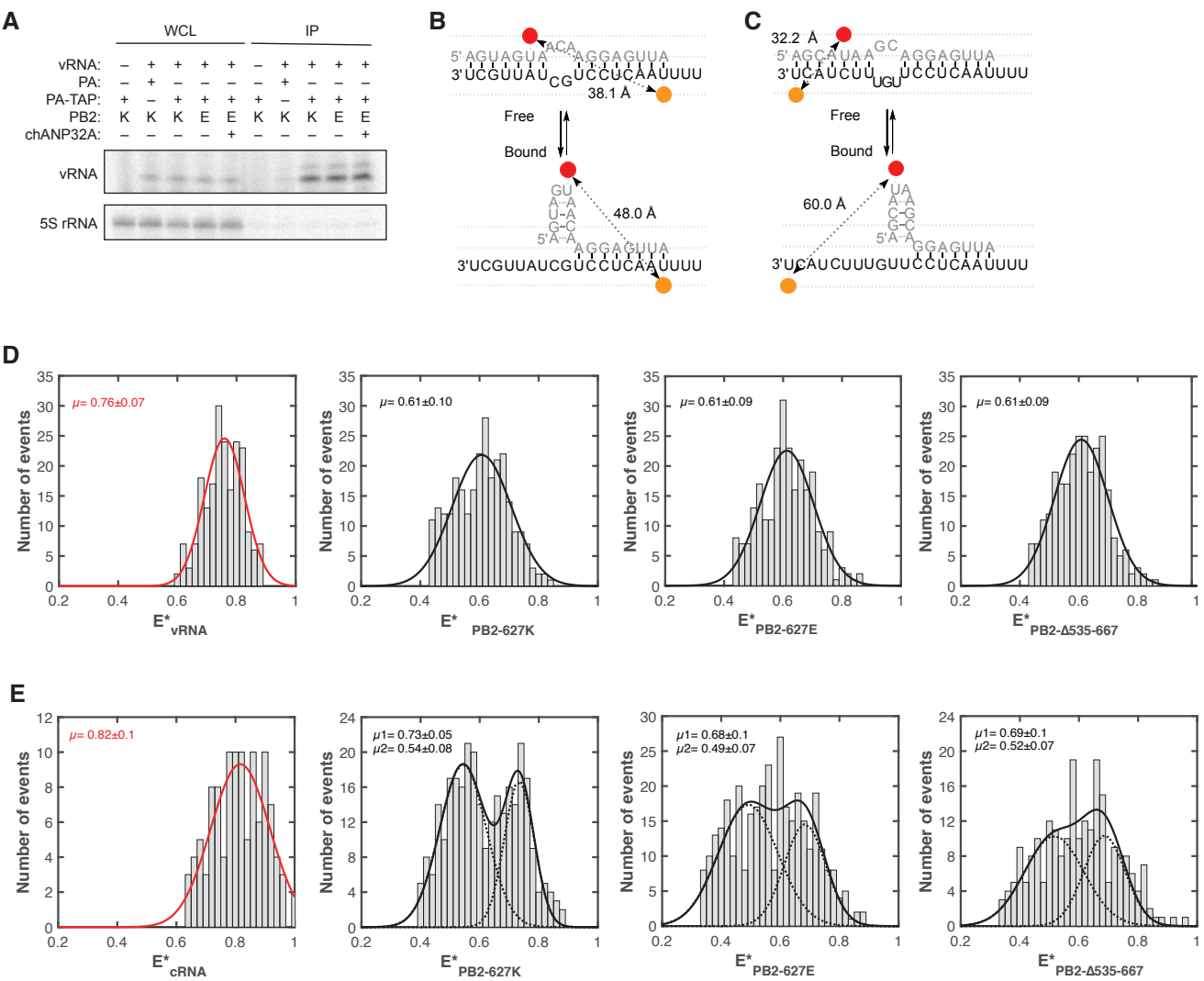
660

661

FIGURE 1
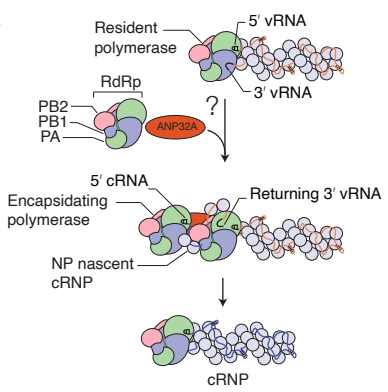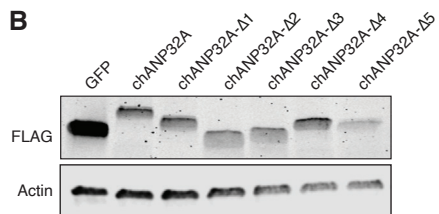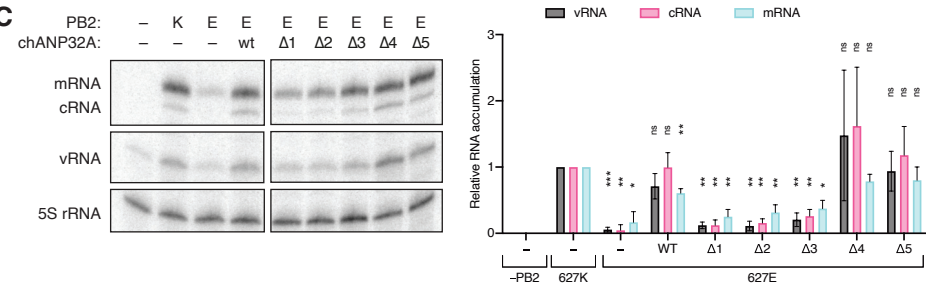
FIGURE 2

FIGURE 3

FIGURE 4

FIGURE 5

A
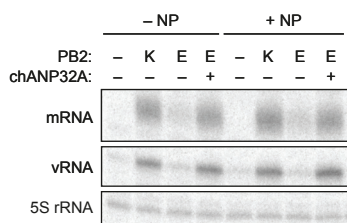
B
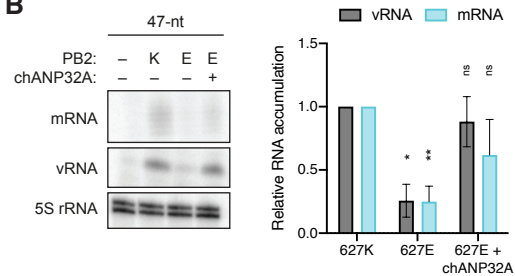
C
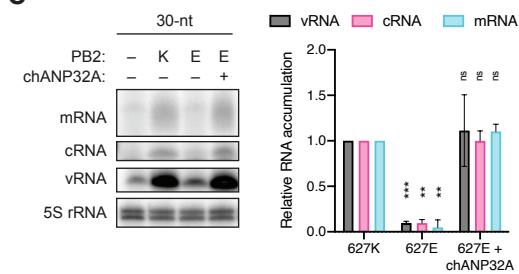
FIGURE 6
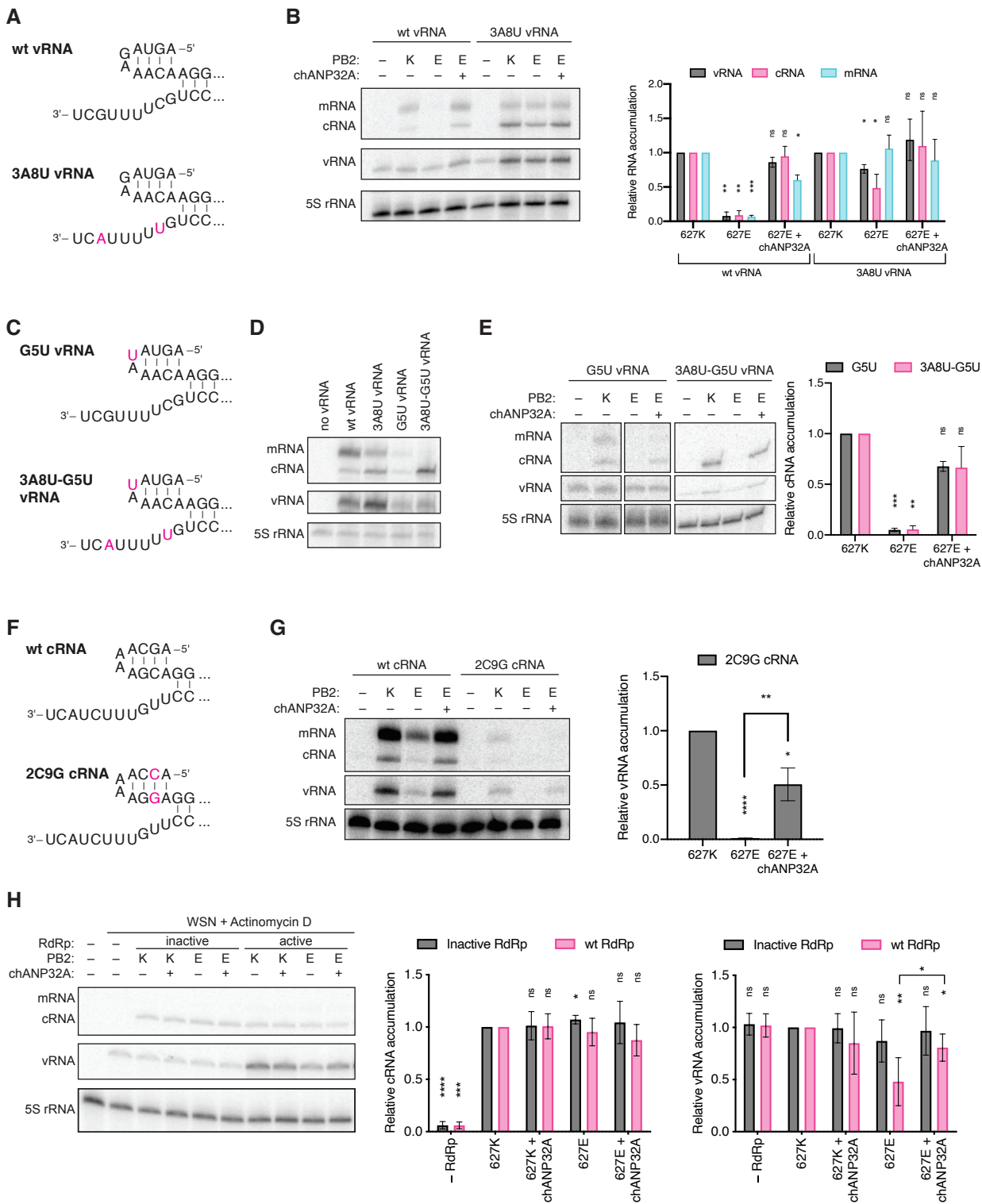
Table 1   **Oligonucleotide sequences**

Mutagenesis primers	Sequence (5' -> 3')
PB2-K627E_F	cgcagccgctccaccagagcaaagtgga
PB2-K627E_R	tccactttgctctggtggagcggctgcg
NA-3A8U_F	gggaccatgccggccagtaaaaacaggagtttaaatgaatc
NA-3A8U_R	gattcatttaaactcctgtttttactggccggcatggtccc
NA-G5U_F	tgttcaaaaaactccttgtttatactaataacccggcggcc
NA-G5U_R	ggccgccgggttattagtataaacaaggagttttttgaaca
cNA-2C9G_F	ggcattttgggccgccgggttattaccaaaaggaggagtttaaatga
cNA-2C9G_R	tcatttaaactcctccttttggtaataacccggcggcccaaaatgcc
NA30_F	ggccagcaaaagcaggagtctccttgtttctactaata
NA30_R	tattagtagaaacaaggagactcctgcttttgctggcc
chANP32AΔ180-208_F	gaggatgtgttgagccttgaagaggagtacgatgac
chANP32AΔ180-208_R	gtcatcgtactcctcttcaaggctcaacacatcctc
chANP32AΔ209-281_F	cgaagaagaagacgaagattaatgataaggatcccccg
chANP32AΔ209-281_R	cggggggatccttatcattaatcttcgtcttcttcttcg
chANP32AΔ220-281_F	acgatgcccaggtcgtataatgataaggatcccc
chANP32AΔ220-281_R	ggggatccttatcattatacgacctgggcatcgt
chANP32AΔ251-281_F	gaggggtataatgacggttaatgataaggatccccc
chANP32AΔ251-281_R	gggggatccttatcattaaccgtcattatacccctc
chANP32AΔ220-250_F	cgatgcccaggtcgtagatgtcgatgacgatg
chANP32AΔ220-250_F	catcgtcatcgacatctacgacctgggcatcg

Primer extension primers	Sequence (5' -> 3')
5S rRNA	TCCCAGGCGGTCTCCCATCC
NA (-)	TGGACTAGTGGGAGCATCAT
NA (+)	TCCAGTATGGTTTTGATTTCCG
NP76 (-)	CAGGGTAGATAATCACTCACAGAG
NP76 (+)	TGATTTCGATGTCACTCTGTGAG
NA47 (-)	GTTCAAAAAACTCCTTGTTTC
NA47 (+)	GAGTTTTTTGAACCATTTAAACTCCTG
NA30 (-)	AGCAAAAGCAGGAGTCTCCTTG
NA30 (+)	GTAGAAACAAGGAGACTCCTGC